NeuroImage 58 (2011) 716–723

Contents lists available at ScienceDirect

NeuroImage

journal homepage: www.elsevier.com/locate/ynimg

A robust cerebral asymmetry in the infant brain: The rightward superior temporal sulcus

H. Glasel [a,b,1], F. Leroy [a,b,1,*], J. Dubois [a,b], L. Hertz-Pannier [b,c,d], J.F. Mangin [b,e], G. Dehaene-Lambertz [a,b]

[a] INSERM, U992, Neurospin, 91191 Gif/Yvette, France, Université Paris 11, Paris, France
[b] IFR49, Neurospin, 91191 Gif/Yvette, France
[c] INSERM, U663, Paris, France; Université Paris 5, Paris, France
[d] CEA, LBIOM, NeuroSpin, Gif-sur-Yvette, France
[e] CEA, LNAO, NeuroSpin, Gif-sur-Yvette, France

ARTICLE INFO

Article history:
Received 21 January 2011
Revised 13 May 2011
Accepted 8 June 2011
Available online 23 June 2011

Keywords:
Infant
MRI
Asymmetry
Brain
Temporal
Language

ABSTRACT

In order to understand how genetic mutations might have favored language development in our species, we need a better description of the human brain at the beginning of life. As the linguistic network mainly involves the left perisylvian regions in adults, we used anatomical MRI to study the structural asymmetries of these regions in 14 preverbal infants. Our results show four significant asymmetries. First and foremost, they stress an important but little-known asymmetry: the larger depth of the right superior temporal sulcus (STS) at the base of Heschl's gyrus. Then, we characterized the early forward and upward shift of the posterior end of the right Sylvian fissure, the elongation of the left *planum temporale* as well as the thickening of the left Heschl's gyrus. The rightward bias of the STS is robust and large, and is not correlated with the leftward asymmetries of the *planum* and Heschl's gyrus, suggesting that different morphogenetic factors drive these asymmetries. As this sulcus is engaged in multiple high-level functions (e.g. language and theory of mind), and has been spotted as abnormal in several developmental disorders (e.g. schizophrenia, autism), this early rightward asymmetry should be further explored as a target for a genetic evolutionary pressure.

Introduction

A striking particularity of the human brain is its asymmetrical organization. Once thought to have been specific of the human species, functional and structural asymmetries have since been described in other mammals and birds (Cantalupo and Hopkins, 2001; Gannon et al., 1998; Gilissen, 2001). However, among mammals, and even within the primate lineage, humans frequently possess the most asymmetrical brain. The main asymmetries observed in the human brain are described as a torque pushing the right frontal area forward and the left occipital region backward (petalias) (Yakovlev, 1962). This twist is combined with a raising and shortening of the right Sylvian fissure relative to the left (LeMay, 1984), creating a prominent shape difference between the left and right posterior temporal regions (Toga and Thompson, 2003; Van Essen, 2005) and a larger left *planum temporale* (Geschwind and Levitsky, 1968).

Because this right-left torsion affects the posterior temporal region, which is involved in elaborate auditory computations among which phonetic representations on the left side, the relation between this macro-structural feature and the emergence of language is a strongly debated question. Other asymmetrical markers have thus been investigated within the auditory and linguistic areas. A larger left inferior frontal region (Broca's area) has been described but the magnitude of the asymmetry is discussed (see Keller et al., 2009 for review). The white matter volume underlying Heschl's gyri is larger on the left than on the right side (Penhune et al., 1996). At the microscopic level, bigger pyramidal cells are reported in the left auditory cortex (Hutsler, 2003) which is also associated with thicker myelinated fibers (Anderson et al., 1999). Asymmetries favoring the right side in the perisylvian regions have also been reported but have drawn less attention and discussion. In particular, four studies (Barrick et al., 2005; Ochiai et al., 2004; Van Essen, 2005; Watkins et al., 2001) have noted a deeper right than left STS in its posterior segment.

In great apes, some of these asymmetries are also found, although to a lesser extent than in humans: a longer left Sylvian fissure (Yeni-Komshian and Benson, 1976), a larger left *planum temporale* (Cantalupo and Hopkins, 2001; Gannon et al., 1998; Gilissen, 2001; Hopkins et al., 2008), and a leftward asymmetry in the inferior frontal regions (Cantalupo and Hopkins, 2001) have been described. By

* Corresponding author at: Laboratoire de Neuroimagerie Cognitive INSERM U992, CEA/SAC/DSV/DRM/NeuroSpin, Bat 145, point courrier 156, F-91191 GIF/YVETTE, France. Fax: +33 1 69 08 79 73.
E-mail address: francois.leroy@cea.fr (F. Leroy).
[1] HG and FL equally contributed to this study.

1053-8119/$ – see front matter © 2011 Elsevier Inc. All rights reserved.
doi:10.1016/j.neuroimage.2011.06.016

contrast, the petalia torque pattern is not observed in chimpanzees while the left occipital petalia is clearly seen in gorillas (Gilissen, 2001). The difference in minicolumn width in humans between left and right *planum temporale* has not been reported in chimpanzees (Buxhoeveden et al., 2001).

From these cross-species comparisons, one can hardly conclude whether a unique genetic factor or a combination of both genetic and environmental parameters drives the asymmetrical features of the human brain. Possible effects include a genetic drift within the primate lineage, a genetic pressure on brain areas involved in communication and linguistic networks as well as environmental changes due to heavy exposure to speech in human. It was indeed suggested that the fast temporal transitions of the speech signal might favor the development of stronger left hemispheric responses because of a bias for processing rapid stimuli in this hemisphere (Boemio et al., 2005; Zatorre and Belin, 2001). Looking at the infant brain, i.e., long before language expertise and handedness develop, should bring useful data in this debate. If asymmetries were present early on in the same regions that would later acquire communication and linguistic skills in adults, they could behave as language-related genetic landmarks and therefore give us crucial insight into the genetic change which occurred between humans and their close cousins in the primate lineage. It could help us understand how this brain reorganization has been critical to promote language emergence in our species.

Studies in infants are still scarce. Post-mortem studies have reported that several right sulci appear one or two weeks earlier than their left counterparts (Chi et al., 1977). The raising and shortening of the right sylvian scissure and a larger left *planum temporale* are also already observed during the fetal life (Chi et al., 1977; Cunningham, 1892; Wada et al., 1975; Witelson and Pallie, 1973). Non invasive brain imaging studies in healthy infants have confirmed an earlier gyration on the right side in preterms (Dubois et al., 2008), a deeper right STS in preterm newborns (Dubois et al., 2010) and a larger left *planum temporale* with a deeper superior temporal sulcus (STS) in full-term neonates (Hill et al., 2010). Studying a large group of neonates, Gilmore et al. (2007) have found that contrary to adults, only one petalia (occipital) is observed and that the left hemisphere is larger than the right. These brain-imaging studies have however been restricted to the neonatal and preterm periods because the study of brain asymmetry is challenging during the first years of life. Specific imaging problems are raised during this period due to the rapid and heterogeneous cerebral maturation that changes white–gray matter contrast, associated with a thin and already highly twisted cortical ribbon. This hampers automatic segmentation of the different brain compartments, which is a major processing step before structural analyses (Leroy et al., submitted for publication). To avoid inaccuracies, manual drawing is thus preferable but limits the number of subjects and structures to be studied.

In this study, we scanned fourteen one to four month-old healthy infants. Author H.G. manually drew the main sulci surrounding the linguistic regions and the central sulcus as a reference. We first assessed that the overall brain and sulcal growth was linear as expected across this age range (Gilmore et al., 2007; Huppi et al., 1998). Second, we reported infant-specific morphology of our structures of interest. We then studied left–right differences in localization and shape of these structures in both normalized and native spaces. Gross asymmetry was measured in the normalized space using linear registration. Because this procedure did not enable to disentangle the respective effects of location, shape and size of the asymmetries, we further analyzed those differences in the native space. We looked for size asymmetry by measuring surface area, length and depth of each structure in the native space. For large structures, e.g. the STS, we analyzed depth variations along the structure.

Materials and methods

Subjects

Fourteen healthy full-term infants (11.1 ± 3.9 weeks, range: 2.6–16.3 weeks; 9 males, 5 females), were included in this study after their parents gave written informed consent. No sedation was used and the infants were systematically asleep during MR imaging. Particular care was taken to minimize the noise exposure, by using customized headphones and by covering the magnet bore with noise protection foam. The study was approved by the regional ethical committee for biomedical research.

Data acquisition and reconstruction

MR acquisitions were performed with a T2 weighted fast spin-echo sequence (TE/TR = 120/5500 ms) on a 1.5 T MRI system (Signa LX, GEMS, USA), using a birdcage head coil. Images covering the whole brain were acquired along the axial, sagittal and coronal orientations for each infant. In each orientation, spatial resolution was $0.8 \times 0.8 \times 2$ mm^3 (field of view: 20 cm, raw matrix: 192×192 interpolated to 256×256). The total acquisition time was 7 min. For each infant, the 3-orientation images were then combined into one high-resolution image of $1 \times 1 \times 1$ mm^3 resolution by using a reconstruction method (Rousseau et al., 2006).

Structures of interest

Delineation in the native space

Structures in the perisylvian regions were manually drawn using Anatomist software (Cointepas et al., 2001). Author H.G. drew the STS, Heschl's gyrus, *planum temporale*, sulci bordering Broca's area (i.e. the inferior frontal sulcus, the inferior precentral sulcus, the anterior ascending and anterior horizontal rami of the Sylvian fissure, and the diagonal sulcus), sulci bordering the supra-marginal gyrus and the central sulcus (Fig. 1A). We defined and systematically delineated a sulcus as the cerebro-spinal fluid space delineated by two sides of gray matter. Drawing was managed slice by slice using a one voxel paintbrush, starting from the outer section of the brain until a wall of gray matter was met. Because sulcation is simpler at this age than in adults, i.e., fewer segments and smoother curvature, a termination based on the adults' sulcus demarcation or on sulcus orientation (given that some sulci such as the right STS are strongly bended) would have been arbitrary and inaccurate. The definition that we chose avoids any top–down biases and was easily applied to all drawn sulci (see Supplementary online material (SOM) for specific description). Drawing was ignorant both of infant age and of the side convention of the acquisitions. When ambiguities were present, final result was discussed with an experienced pediatric neuroradiologist (H-P. L.).

In order to assess drawing reliability, we further computed automatic sulci delineation on a subset of subjects and compared automatic and manual sulci drawing. Automatic and manual sulcal surfaces were highly correlated (correlation = 0.97) (see SOM for further details).

Size measurement

Once drawn, a smooth 3D shape of the structure was created using a triangulation method (Fig. 1A) (maximum mesh clearance of 5 mm). Structure surface area, length and maximum depth were computed using Brainvisa software (Cointepas et al., 2001).

Local depth was also computed along most sulci, as the local geodesic distance between the most inner sulcal voxel and the closest sulcal voxel to the brain envelope. Local measurement was repeated across the whole structure in order to produce a depth profile, i.e., depth variation along the sulcus. For the STS, the profile included only the axis parallel to the Sylvian fissure, i.e. the horizontal branch and its prolongation in the

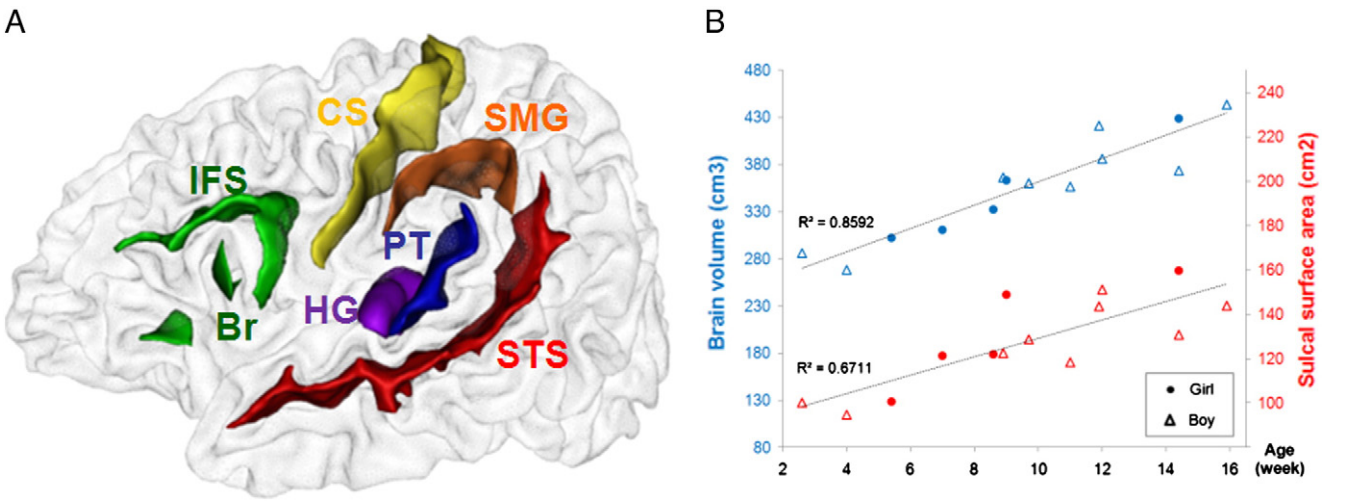

Fig. 1. Sulcus drawing and overall brain and sulcal growth. A. The main perisylvian sulci have been manually drawn, and then a 3D shape of the structure was created. STS: superior temporal sulcus, PT: *planum temporale*, HG: Heschl's gyrus, SMG: supra-marginal gyrus, IFS: inferior frontal sulcus, Br: Broca rami, CS: central sulcus. B. Expected linear growth of brain volume and sulcal surface area with age. Once normalized, sulcal surface area did no longer change with age. In our dataset, no difference of global growth was seen between boys and girls.

anterior ascending terminal branch surrounded by the supra-marginal gyrus. Depth profiles along Broca's rami and the sulci bordering the supra-marginal gyrus were not computed because of either the small size or the highly variable shape of these structures.

As for Heschl's gyrus, the initial delineation was a gutter-like structure made of cortical voxels only. We applied a closing operator (10 mm wide) of mathematical morphology over this segmentation. As a result, all voxels between the gutter sides, i.e., gyral white matter, were added to the segmentation. The whole Heschl's gyrus, including gray and white matters, was obtained through this mathematical transformation. We then measured its volume and its mean cross-section.

Finally, to take into account the brain growth during the age range considered, we normalized each measurement, i.e., surface area (S), length (L) and depth (D), by the infant's brain surface. We first segmented the rough interface between white and gray matters with an approach specific of immature brains (Leroy et al. (submitted for publication)). We then applied a morphological closing of 10 mm to get a smooth envelope of each cerebral hemisphere using BrainVISA software. The surface areas (S_H) of left and right hemispheric envelopes were used for normalization. Specifically, normalizations for both two-dimensional and one-dimensional measurements were given by: $S_N = S/S_H$; $L_N = L/(S_H)^{0.5}$; $D_N = D/(S_H)^{0.5}$ computed in each subject.

Structure landmark

A landmark was set for each structure to match their profiles across subjects. For the *planum temporale*, we chose its deepest location, which is easily located near the insula as the inner vertex of the *planum's* triangular shape. The distance from this location to the central landmark used in Caret software for brain analysis (Van Essen, 2005), i.e., the lower endpoint of the central sulcus, was relatively stationary across subjects (Table 1), whereas the same measurements for the two other vertices of its triangular shape were more variable. Moreover, internal parts of folding patterns are considered more stable than external parts (Lohmann et al., 1999; Régis et al., 2005). We projected a vertical virtual line from the *planum* origin on the STS and it set the STS reference origin. For Heschl's gyrus, the reference was set at the most posterior and medial location, since the koniocortical core covers approximately the medial 2/3 of the gyrus (von Economo and Koskinas, 1925). For the central sulcus, we chose the motor hand landmark whose cortical MRI signal is darker than surrounding regions in the infant brain. More precisely, the reference origin was set at the lateral end of the middle genu on the surface of the sulcus (Yousry et al., 1997). For the precentral inferior frontal structure, the origin was set at the junction between the horizontal inferior frontal sulcus and the vertical precentral sulcus.

Statistical analyses

Analyses in the normalized space

In order to get a general idea of the left–right differences in the location and geometry of the sulci, we first performed an analysis of the binary masks of each structure in a normalized space (Fig. 2). In each subject, each manually delineated structure was transformed in a binary image including its left and right parts (structural masks). Individual high resolution T2-weighted image was normalized to an anatomical infant template (Dehaene-Lambertz et al., 2002) using a linear transformation. The transformation parameters were applied to the infant's masks (S). The original masks were then flipped along the left–right axis (fS) to obtain mirror images. Our goal with this simple flip was to preserve any left–right geometrical differences (e.g. a shorter right Sylvian fissure). Original and flipped masks were smoothed with a 5-mm Gaussian filter. Because sulci are very elongated structures, the filter size was large enough to enhance overlap between ipsilateral sulci while preserving detection of left–right differences. For each structure, we then performed a voxel-by-voxel analysis with Statistical Parameter

Table 1
Euclidean distance asymmetry between landmarks.

Distance		Left (mm)		Right (mm)		AI		One-tailed (L>R)	
From	to	Mean	SE	Mean	SE	Mean	SE	t(13)	p
IFS	CS	16.2	1.6	13.8	1.0	−13.4%	10.0%	1.35	0.1008
	HG	25.7	1.4	23.9	0.7	−5.8%	5.1%	1.15	0.1347
	iPT	38.8	0.9	34.7	0.9	−11.4%	2.7%	4.25	0.0005
	pPT	40.1	1.6	32.6	1.6	−21.3%	5.3%	4.02	0.0007
	pSTS	55.3	2.2	49.0	2.0	−12.1%	3.7%	3.30	0.0028
CS	HG	18.7	0.7	17.6	0.6	−6.2%	5.4%	1.14	0.1366
	iPT	30.7	0.5	28.5	0.6	−7.5%	2.1%	3.58	0.0017
	pPT	28.3	1.4	23.6	1.2	−18.2%	4.1%	4.49	0.0003
	pSTS	43.9	1.8	39.9	1.7	−9.6%	3.9%	2.48	0.0138
pPT	HG	33.1	2.0	30.1	1.2	−8.4%	4.5%	1.86	0.0430
	iPT	22.5	1.5	20.0	1.0	−10.4%	6.3%	1.64	0.0626
	pSTS	19.8	1.9	19.0	2.0	−6.0%	11.7%	<1	–

AI, asymmetry index (>0 is rightward); SE, standard error; L, left; R, right; CS: central sulcus; IFS: junction between inferior frontal sulcus and precentral sulcus; HG, anterior point of Heschl's gyrus; i/pPT, inner/posterior tips of *planum temporale*; pSTS, STS posterior end. See Fig. 3 for location of these landmarks.

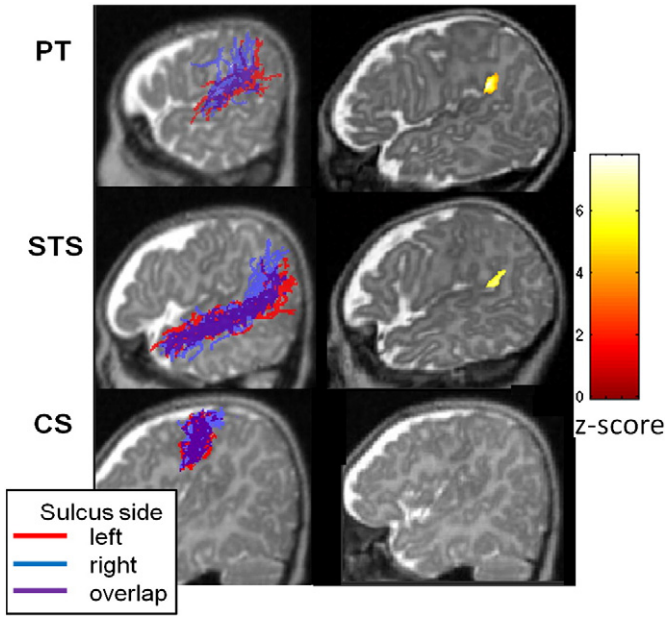

Fig. 2. Topographical asymmetries: Analyses in a normalized space reveal the difference in location of the STS and *planum temporale* (PT), related to a steeper and shorter right sylvian fissure. No difference is noticeable for the central sulcus, the supra-marginal and frontal sulci. The 14 left (red) and right (blue) individual sulci are presented on sagittal slices of an individual infant (left) on the left; on the right voxel-by-voxel statistical values two superior and inferior clusters in PT and one posterior cluster in the STS are detected (voxel $p<0.001$, cluster $p<0.05$ corrected for multiple comparison).

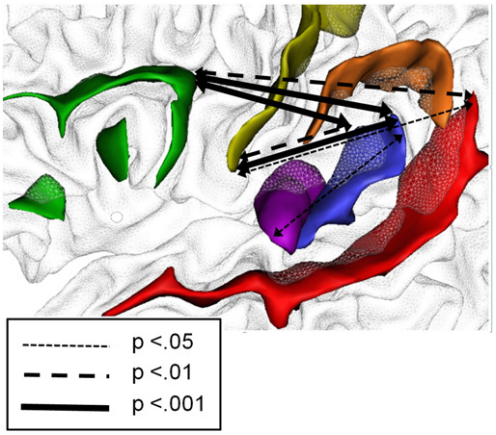

Fig. 3. Distance asymmetries over a lateral view of the posterior temporal regions. Euclidian distances are measured from the posterior temporal regions to both the lateral tip of the central sulcus and the junction of the inferior frontal–precentral sulci. Asymmetries are leftward, related to an elongated left *planum temporale* and further increased by the greater distance between the left precentral and central sulci.

Mapping software (SPM2, FIL, http://www.fil.ion.ucl.ac.uk/spm) by carrying on a paired *t*-test comparison between the original and the flipped images across infants. Because of their relatively small sizes and their common border, the *planum temporale* and Heschl's gyrus were studied together. Other structures were analyzed separately in order to avoid overlaps, e.g. the right STS with the left *planum temporale*. As the analysis mask was the sum of all individual masks, its volume was related to the structure size and to its spatial variations across subjects (STS: 392 272 mm^3, *planum temporale* and Heschl's gyrus: 170,976 mm^3, SMG sulci: 193,638 mm^3, Broca's sulci: 218,100 mm^3, central sulcus: 240,000 mm^3). Clusters were reported when voxels were significant at $p<0.001$ and formed a contiguous cluster whose extent was significant at $p<0.05$.

Native space analyses

We examined left–right differences in sulcal location and size (surface, length and depth).

Relative position. In adults, the most robust asymmetry concerns the posterior temporal structures, particularly the *planum temporale* (Geschwind and Levitsky, 1968). To better understand the geometry of this region in infants, we measured 3D distances in the native space of each infant among the following locations: the bottom of the central sulcus (CARET landmark, (Van Essen, 2005)), the junction between the inferior frontal sulcus and the inferior part of the precentral sulcus (easily detected as the maximum curvature point along the sulcus), the three endpoints of the triangular *planum temporale* as well as the posterior end of the STS (see Fig. 3 and Table 1). All distances were normalized to the surface area of the ipsilateral hemispheric envelope, and an asymmetry index (AI) was computed: $AI = 2\ (D_{right} - D_{left})/(D_{right} + D_{left})$, with D, the Euclidean distance between two brain locations. We tested whether this index was significantly different from zero in the same direction than reported in the adult literature using one tailed Student t-tests.

Size. Normalized asymmetry indices were computed for the sulcal surface area, length and depth. We tested whether these indices were significantly different from zero using two-tailed Student t-tests across infants. For long sulci, we estimated the most asymmetrical depth segment using permutation tests. First, we computed the paired t score between right and left profiles at each sulcal location using a sliding window and determined the most asymmetrical segment which provided the maximum t score (reported as t_{max} in the results section). Then, 2^n random inversions of right and left profiles across the *n* subjects were performed to estimate the random distribution of t score maximal values. Finally, the measured t_{max} was compared to this distribution to obtain the p corrected value. We first detected asymmetrical segments using a 5 mm-wide sliding window and then increased the window size up to 20 mm to get its full spatial scope.

Results

Global growth and shape of brain and regions of interest

Over this short developmental period, the brain growth was linear (12 cm^3 volume increase per week using standard linear regression analysis, $R^2 = 0.86$) and close to the neonates' brain growth during the 38–48 weeks of gestation period (Gilmore et al., 2007). The surface area of the brain envelope and sulci also increased linearly with age and no difference was seen between males and females in our dataset (Fig. 1B). Once normalized to the brain envelope, sulcal surface area no longer changed with age, which suggests that the folding process was neither faster nor slower than the overall growth of the brain. Furthermore, there was no overall inter-hemispheric asymmetry, neither in the surface area ($p = 0.11$) nor in the volume of the hemispheres ($t<1$, see Table 2 SOM for more details).

The sulcation was simpler than in adults. Sulci had less tertiary branches, and those which are broken into segments in adults (e.g. the STS), were often continuous in this age range. The right STS was not segmented and two left STS were made of two segments (2/14). The inferior frontal sulcus was connected to the inferior precentral sulcus in all but one infant. Finally, only three Heschl's gyri were duplicated (3/28). (Fig. 1 SOM).

Normalized space analyses: Relative positions of right and left structures

The voxel-by-voxel analyses of the binary masks of the structures revealed asymmetries in the STS and the Heschl's gyrus—*planum temporale* while no significant cluster was observed for the sulci

bordering Broca's area and the supra-marginal gyrus, nor for the central sulcus (Fig. 2). By focusing qualitatively on each infant structure, we observed that the right *planum* was more anterior and oblique than its left counterpart, which was more horizontal. This asymmetry in relative positions likely drove our results (superior cluster of 3319 voxels, $p_{cor}<0.001$; inferior cluster of 732 voxels, $p_{cor}<0.001$). Similarly the right STS was more dorsal and anterior than the left one (cluster of 482 voxels, $p_{cor}=0.001$).

Native space analyses: 3D distances between landmarks

We measured asymmetrical distances between landmarks in the posterior regions of the Sylvian fissure in infants (Fig. 3 and Table 1). Heschl's anterior and posterior limits were equally distant from the central sulcus reference on both sides. By contrast, the distance to the central sulcus increased for structures behind Heschl's gyrus on the left side, i.e., the inner vertex of the *planum* ($p=0.002$) and the end points of both the Sylvian fissure ($p=0.0003$) and the STS ($p=0.014$). Part of the posterior temporal asymmetry was thus related to an elongated left *planum*. The distance between the precentral–inferior frontal sulcus junction and the central sulcus reference was slightly larger on the left (13.4%), although it was not significant ($p=.10$). Thus, instead of compensating for the posterior asymmetry, this tendency contributes to a distance increase between the frontal and posterior linguistic regions on the left side (see Table 1). None of these normalized distances correlated with age, which suggests that this spatial organization is stable during the first post-natal weeks.

Native space analyses: Surface area, length and depth of regions of interest

The distances presented above are affected by the sulcal shape, which can be more or less bended. Therefore, we also measured the surface area, length and depth of the significant asymmetric structures (Fig. 4 and also Table 2 SOM). The STS surface was greater on the right than on the left (18%, $p=0.017$), and most of its asymmetry was explained by a rightward bias in depth (20%, $p=0.001$). Its depth on the right side increased with age ($R^2=0.32$, $F(1,12)=5.66$, $p=0.035$). The STS was the only structure with a rightward asymmetry, and its right depth was the only feature to increase with age after normalization by the cortical envelope.

By contrast, the *planum temporale* surface area tended to be larger on the left (−15%, $p=0.065$), due to a leftward elongation (−15%, $p=0.048$). Although a larger left *planum* and a larger right STS were present in most infants (respectively 10 and 11 infants over 14), there was no correlation between the asymmetry indices of both structures ($R^2=0.008$). Heschl's gyrus was thicker on the left side (mean cross-section: −25.4%, $p=0.023$). Again, there was no correlation between both leftwards asymmetries of the *planum* and Heschl's gyrus.

Native space analyses: Localization of depth asymmetry

For the larger sulci, we computed the depth profile along their main axis (Fig. 5). The deepest points of bilateral STS were both located at the base of the *planum temporale* inner vertex ($x=+2$ mm along the axis). Anterior to this deepest point and therefore to the *planum temporale*, a 15 mm-long segment was significantly deeper on the right than on the left (39% difference over [−21 mm,−7 mm]: $t_{max}=4.29$ $p_{cor}=0.002$). This rightward asymmetry was present in 12 of the 14 infants. A leftward asymmetry observed at the junction between the inferior frontal sulcus and the precentral sulcus did not reach significance at a p corrected level (−17% over [−1,+3 mm]: $t_{max}=1.9$ $p_{cor}=0.22$). No depth asymmetry was observed along the *planum temporale* and central sulci.

Discussion

To summarize our main results, we observed major structural asymmetries in the posterior perisylvian regions in human infants during the first post-natal months. Analysis in a normalized space

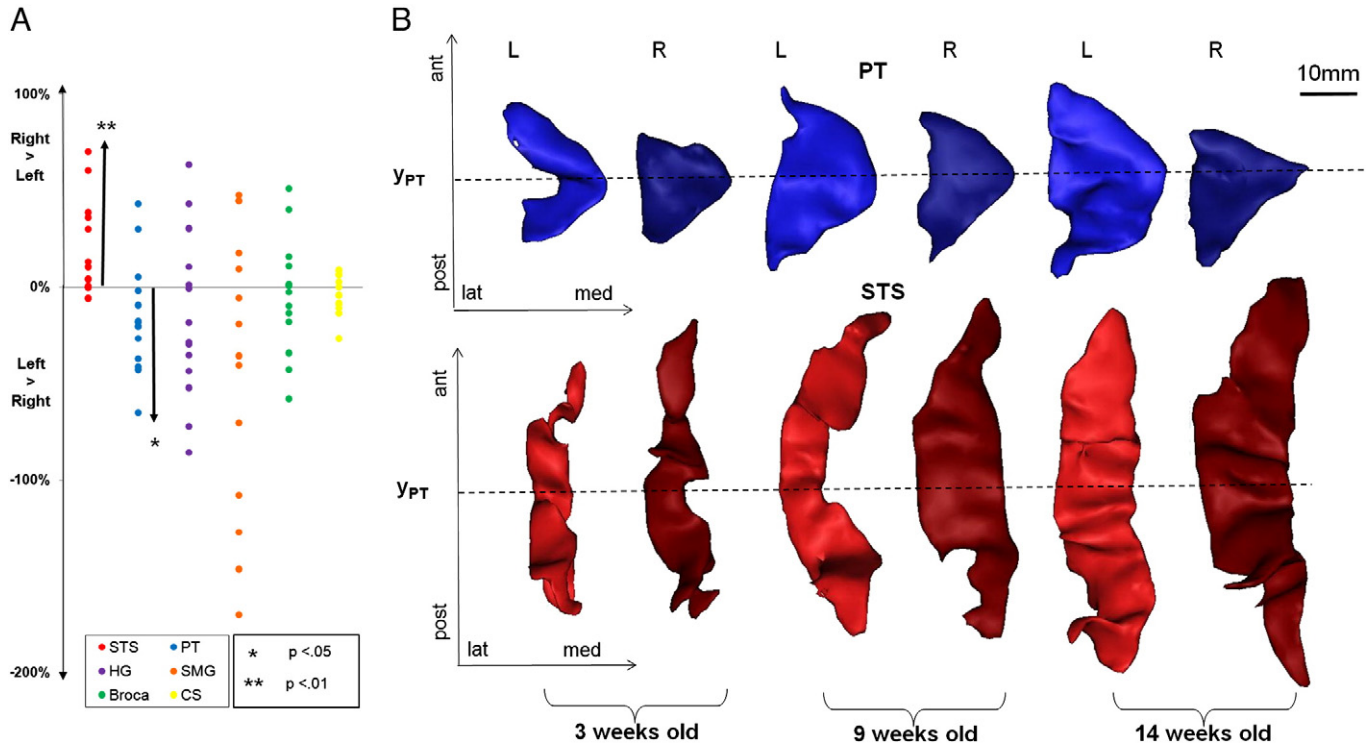

Fig. 4. Structure asymmetry. A. Surface asymmetry (in percent) after normalization to the hemispheric white matter envelope. B. Left and right sulci from three infants; Asymmetry of PT (top row) and STS (bottom row). Structures are seen from above the superior temporal plane. Right sulci are darker than the left ones. The horizontal dashed lines show the coronal coordinate of the inner tip of each planum temporale (y_{PT}).

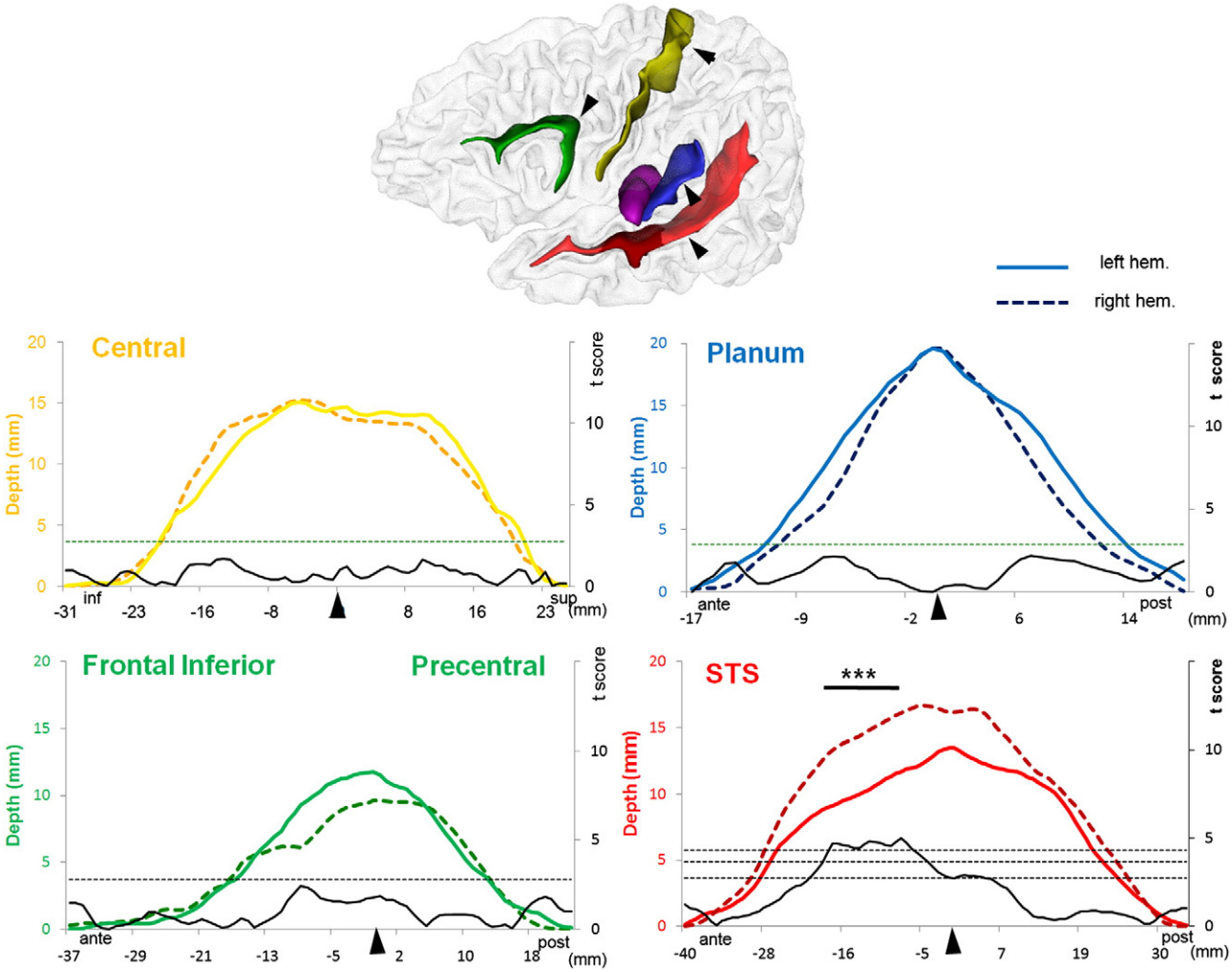

Fig. 5. Depth variation along sulci. Left (right) depth profiles are shown in light colored continuous lines (dark colored dashed lines), respectively; *t*-test score is shown in black; dashed black lines give successive statistical thresholds using permutations (first line: p = 0.05; upper second line: p = 0.01; upper third line: p = 0.005). Location of the rightward STS asymmetry is shown in dark red on the 3D brain mesh. Black arrowheads set sulcal origin. Depth is normalized to the hemispheric white matter envelope.

showed the classical forward and upward shift of the right posterior corners of the Sylvian fissure and STS relative to the left. Our measures in the native space went beyond this topographical asymmetry, and demonstrated shape and size differences for the posterior Sylvian fissure and the STS. The *planum temporale* length and Heschl's gyrus thickness were larger on the left side. Primarily, this study emphasized the lesser known asymmetry of the STS depth.

A major asymmetry in infants: A deeper right STS

The rightward STS asymmetry was as large as the classical leftward asymmetry of the *planum temporale,* in both size and reproducibility across subjects. For both structures, we found 14–18% of size difference, and asymmetry concerned ten to eleven infants (over 70%) and even 100% of the infants for the STS if we consider only the segment parallel to the Sylvian fissure without its posterior branch.

Because most of the sulci appear first on the right side in humans (Chi et al., 1977; Dubois et al., 2008), the STS asymmetry in our infants might be related to the right hemisphere being ahead of the left one, which would later weaken and vanish when the folding pattern develops and catches up in the left hemisphere. Instead, we suggest that this asymmetry represents an important structural characteristic of the human brain. Two arguments sustain this hypothesis.

First, the STS appears relatively early during fetal development. Its posterior section is noticed between 23 and 30 weeks of gestation (Dubois et al., 2008; Kasprian et al., 2011). It appears earlier than the inferior frontal and the intra-parietal sulci for example (Chi et al., 1977). Yet these sulci are symmetrical in our infant group. The central sulcus, which also appears first on the right side (Chi et al., 1977) around 18–20 weeks of gestation, is already reported as symmetric eight–ten weeks later in the younger maturational age (26–28 weeks of gestation) (Dubois et al., 2008). Thus, the left sulcation, which is initially delayed, seems to catch up within a few weeks. If the STS was following the same general pattern, its asymmetry would no longer be visible in post-term infants. By studying the brain folding patterns in a normalized space in full-term neonates, Hill et al. (2010) did not observe any significant rightward asymmetry. However, when the STS was manually traced in each neonate, it was 1.7 mm deeper on the right side. Here in our 3-month-old infants, it is around 4 mm deeper and the depth of the right STS is the only feature which increases faster than the general growth of the brain.

Second, the STS asymmetry has also been reported in the adult brain. Delineation of the STS by Ochiai et al. (2004) in 24 adults has shown the forward location of the posterior end of the right STS relative to the left and a deeper right sulcus in its posterior segment. Using surface-based analyses, Van Essen (Van Essen, 2005) has also reported left–right asymmetries in sulcal depth in two groups of 12

adults: 3 to 9 mm deeper on the right for the STS, and 4 to 7 mm deeper on the left for the *planum temporale*. Using inter-atlas registration between the PALS-B12 atlas and a newly designed infant atlas, Hill et al. (2010) have shown that the asymmetrical segment was at a similar location in neonates and adults, i.e. close to the *planum temporale*. Furthermore, Watkins et al. (2001) studied structural asymmetries in 142 young adults using voxel-based morphometry. They observed two clusters of gray matter in the depth of the STS which are larger on the right side, one approximately at the base of the Heschl's gyrus and the other under the *planum temporale* ($x=40$, $y=-29$, $z=-3$ in Talairach coordinates). A cluster close to the latter ($x=49$, $y=-36$, $z=7$) has also been found by Barrick et al. (2005) in 30 young adults. These observations confirm that the STS asymmetry is not solely a characteristic of the preterm brain.

The depth difference of the STS has not been reported in such details as the well-known asymmetry of the *planum temporale* for at least two reasons. First, it might have been missed in *post-mortem* studies because it is a buried feature, which is difficult to measure and can be revealed only by unfolding the cortical surface. Second, this local asymmetry can be blurred in global neuro-imaging analyses. In neonates, the STS asymmetry was not detected using a surface-based approach but was reported after having precisely delineated the structure (Hill et al., 2010). In adults, Im et al. (2010) have reported a high spatial variability of sulcal landmarks in the right posterior STS region. Furthermore, inverse surface asymmetries in the posterior temporal region, i.e., a larger left *planum temporale* combined with a higher right sylvian fissure and a deeper right STS, might cause greater inaccuracies for comparing left and right structures.

Consequently, a deeper right STS seems an important asymmetric feature of the human brain across the lifespan. However, further studies are needed to characterize its developmental trajectory during childhood and adolescence.

To our knowledge, the depth asymmetry of the STS has not been reported in non-human primates. Hopkins et al., 2000 have studied the Sylvian fissure and STS in monkeys and chimpanzees (2000). They reported a longer right STS in monkeys but not in apes. Although the STS length was measured at different sulcal depth, it is not possible to compare their measure with ours. In a recent voxel-by-voxel study in the chimpanzee brain, Hopkins et al. (2008) have reported several asymmetric regions, but none in the STS. However, as discussed above, this asymmetry is difficult to see with a traditional voxel-by-voxel approach, and needs to use a sulcus-based procedure such as in BrainVisa (Mangin et al., 2004).

Further characterization of asymmetry in the posterior temporal region

In addition to the STS asymmetry, we characterized the well-known asymmetry of the posterior temporal region. Whereas Heschl's endpoints were at equal distance from a central reference point, locations posterior to Heschl's gyrus were further away from the central reference on the left side than on the right side (Fig. 3). This asymmetry could be explained by the forward and upward shift of the right Sylvian fissure (Fig. 2) as well as an increase in the left cortical surface behind Heschl's gyrus.

Because the posterior end of the sylvian fissure is often smoothly bended in the infant brain, we drew the *planum* posteriorly until we met a cortical wall thus including both horizontal and vertical end segments of the Sylvian fissure. We observed that both its surface area and its length tended to be greater on the left side. In neonates, Hill et al. (2010) also reported that this region was 3 mm deeper on the left. This structural asymmetry sustains functional asymmetries. In a recent experiment, we have shown that speech stimuli elicited significantly stronger responses than music in the left *planum temporale* in two-month-old infants (Dehaene-Lambertz et al., 2009) whereas Perani et al. (2010) observed better discrimination capacities for music stimuli in the neonates' right *planum temporale*.

Other structural observations

Other asymmetries within the language network have been described in the adult brain, such as a larger left Heschl's gyrus and a larger Broca's area. In our infants, left Heschl's gyrus was thicker with a larger volume. A larger gyrus is consistent with thicker cortical layers and larger white matter bundles on the left side (Penhune et al., 1996). We did not observe asymmetries in the inferior frontal region. Our method applied to the sulci bordering Broca's area is merely a first approach to characterize this region, and gyral parts should certainly be taken into account. We observed a tendency for a deeper left sulcus at the junction between the precentral and the inferior frontal sulcus, but it did not reach significance at a corrected level. Further studies should reconsider this issue with older infants to see whether this leftward depth difference increases with age and with the development of language production.

Asymmetries: A target for genetic studies

The asymmetrical development of the human brain within perisylvian regions can be characterized by four features as consistent in infant as in adult: the forward and upward shift of the posterior end of the right Sylvian fissure, the enlargement of the left *planum temporale*, the thickening of Heschl's gyrus, and the depth increase of the right STS. They might result from complex interactions between asymmetrical expressions of morphogenetic factors and fiber connectivity constraints. Several genes with an asymmetric expression in the human brain have been described. For example, LMO4 is asymmetrically expressed toward the right side in the human brain between 12 and 14 weeks of gestation (Sun et al., 2005). Although other gene expressions are symmetric during convolution development at a global population-level (Johnson et al., 2009), 76% of human genes are expressed in the fetal brain from 18 to 23 weeks of gestation, and 44% of these are differentially regulated. It creates an intricate patchwork of brain regions with complex interactions and possibly local asymmetrical gene expression that can regulate the size of the subventricular zone (Kriegstein et al., 2006). The absence of correlation between the asymmetry of the *planum temporale*, Heschl's gyrus and STS, as the high spatial variability of the folding pattern in the posterior temporal regions reported in newborns (Hill et al., 2010) might be related to separate gene expressions in these regions. Nevertheless, the consistent and localized asymmetry in the STS depth, at the base of Heschl's gyrus, might be a useful target for understanding morphogenetic processes and gene regulation in the human brain.

Finally, interactions between long-range and short-range fiber connectivity produce additional mechanical constraints (Van Essen, 1997), that could modulate the depth difference in the STS. During fetal age, projection fibers accumulate in the subplate zone that is well developed in the cortical gyri but reduced in the bottom of the sulci (Vasung et al., 2010). Using diffusion tensor imaging in a previous study in infants (Dubois et al., 2009), we were able to reconstruct the arcuate fasciculus, i.e. the main white matter fasciculus connecting temporal and frontal regions, and to detect a larger left volume of fibers in the temporal region. Such white matter asymmetry might contribute to the sulcal difference we reported here.

Conclusion

The asymmetrical features that we have uncovered in this study emphasize the particular structural organization of the human brain from early on. The consistency of these features in humans early on accounts for further research in their positive effects on a developing brain. The increase in size of the left *planum temporale* and Heschl's

gyrus have been related to a better processing of fast temporal transitions in these left regions, whereas right regions would be more efficient for spectral coding (Boemio et al., 2005; Zatorre and Belin, 2001). Several functional results in infants showing early left–right processing biases depending on the acoustic features of auditory stimuli are consistent with this hypothesis (Dehaene-Lambertz et al., 2009; Perani et al., 2010; Telkemeyer et al., 2009). The functional significance of a deeper right STS is not fully understood. A larger right volume in the depth of the STS might favor right hemispheric regions involved in theory of mind, voice perception, biological motion perception and visual processing. Conversely, a shallower left sulcus might provide language with a more convenient organization. Further studies are needed to better understand how the asymmetry of the STS favors differential development in regions strongly involved in both verbal and non verbal human social communication.

Acknowledgments

The authors thank Mr Brunet from Ravier-Touzard Company for designing a baby bouncer chair specifically adapted to the head coil, F. Brunelle for the support, F Rousseau for sharing his softwares, the McDonnell foundation, La Fondation Motrice and ANR for financial support to this research, ENP and Fyssen Fundation for funding J.D.

Appendix A. Supplementary data

Supplementary data to this article can be found online at doi:10.1016/j.neuroimage.2011.06.016.

References

Anderson, B., Southern, B.D., Powers, R.E., 1999. Anatomic asymmetries of the posterior superior temporal lobes: a postmortem study. Neuropsychiatry Neuropsychol. Behav. Neurol. 12, 247–254.
Barrick, T.R., Mackay, C.E., Prima, S., Maes, F., Vandermeulen, D., Crow, T.J., Roberts, N., 2005. Automatic analysis of cerebral asymmetry: an exploratory study of the relationship between brain torque and planum temporale asymmetry. NeuroImage 24, 678–691.
Boemio, A., Fromm, S., Braun, A., Poeppel, D., 2005. Hierarchical and asymmetric temporal sensitivity in human auditory cortices. Nat. Neurosci. 8, 389–395.
Buxhoeveden, D.P., Switala, A.E., Litaker, M., Roy, E., Casanova, M.F., 2001. Lateralization of minicolumns in human planum temporale is absent in nonhuman primate cortex. Brain Behav. Evol. 57, 349–358.
Cantalupo, C., Hopkins, W.D., 2001. Asymmetric Broca's area in great apes. Nature 414, 505.
Chi, J.G., Dooling, E.C., Gilles, F.H., 1977. Gyral development of the human brain. Ann. Neurol. 1, 86–93.
Cointepas, Y., Mangin, J.F., Garnero, L., Poline, J.B., Benali, H., 2001. BrainVISA: software platform for analysis of multi-modality brain data. NeuroImage 13, S98.
Cunningham, D.J., 1892. Contribution to the Surface Anatomy of the Cerebal Hemispheres. Royal Irish Academy, Dublin.
Dehaene-Lambertz, G., Dehaene, S., Hertz-Pannier, L., 2002. Functional neuroimaging of speech perception in infants. Science 298, 2013–2015.
Dehaene-Lambertz, G., Montavont, A., Jobert, A., Allirol, L., Dubois, J., Hertz-Pannier, L., Dehaene, S., 2009. Language or music, mother or Mozart? Structural and environmental influences on infants' language networks. Brain Lang. doi:10.1016/j.bandl.2009.09.003.
Dubois, J., Benders, M., Cachia, A., Lazeyras, F., Ha-Vinh Leuchter, R., Sizonenko, S.V., Borradori-Tolsa, C., Mangin, J.F., Huppi, P.S., 2008. Mapping the early cortical folding process in the preterm newborn brain. Cereb. Cortex 18, 1444–1454.
Dubois, J., Benders, M., Lazeyras, F., Borradori-Tolsa, C., Ha-Vinh Leuchter, R., Mangin, J.F., Hüppi, P.S., 2010. Structural asymmetries of perisylvian regions in the preterm newborn. NeuroImage 52, 32–42.
Dubois, J., Hertz-Pannier, L., Cachia, A., Mangin, J.F., Le Bihan, D., Dehaene-Lambertz, G., 2009. Structural asymmetries in the infant language and sensori-motor networks. Cereb. Cortex 19, 414–423.
Gannon, P.J., Holloway, R.L., Broadfield, D.C., Braun, A.R., 1998. Asymmetry of chimpanzee planum temporale: humanlike pattern of Wernicke's brain language area homolog. Science 279, 220–222.
Geschwind, N., Levitsky, W., 1968. Human brain: left–right asymmetries in temporal speech region. Science 161, 186–187.
Gilissen, E., 2001. Structural symmetries and asymmetries in human and chimpanzee brains. In: Falk, D., Gibson, K.R. (Eds.), Evolutionary Anatomy of the Primate Cerebral Cortex. Cambridge University Press, Cambridge, pp. 187–215.
Gilmore, J.H., Lin, W., Prastawa, M.W., Looney, C.B., Vetsa, Y.S., Knickmeyer, R.C., Evans, D.D., Smith, J.K., Hamer, R.M., Lieberman, J.A., Gerig, G., 2007. Regional gray matter growth, sexual dimorphism, and cerebral asymmetry in the neonatal brain. J. Neurosci. 27, 1255–1260.
Hill, J., Dierker, D., Neil, J., Inder, T., Knutsen, A., Harwell, J., Coalson, T., Van Essen, D., 2010. A surface-based analysis of hemispheric asymmetries and folding of cerebral cortex in term-born human infants. J. Neurosci. 30, 2268–2276.
Hopkins, W.D., Pilcher, D.L., MacGregor, L., 2000. Sylvian fissure asymmetries in nonhuman primates revisited: a comparative MRI study. Brain Behav. Evol. 56, 293–299.
Hopkins, W.D., Taglialatela, J.P., Meguerditchian, A., Nir, T., Schenker, N.M., Sherwood, C.C., 2008. Gray matter asymmetries in chimpanzees as revealed by voxel-based morphometry. NeuroImage 42, 491–497.
Huppi, P.S., Warfield, S., Kikinis, R., Barnes, P.D., Zientara, G.P., Jolesz, F.A., Tsuji, M.K., Volpe, J.J., 1998. Quantitative magnetic resonance imaging of brain development in premature and mature newborns. Ann. Neurol. 43, 224–235.
Hutsler, J.J., 2003. The specialized structure of human language cortex: pyramidal cell size asymmetries within auditory and language-associated regions of the temporal lobes. Brain Lang. 86, 226–242.
Im, K., Jo, H.J., Mangin, J.F., Evans, A.C., Kim, S.I., Lee, J.M., 2010. Spatial distribution of deep sulcal landmarks and hemispherical asymmetry on the cortical surface. Cereb. Cortex 20, 602–611.
Johnson, M.B., Kawasawa, Y.I., Mason, C.E., Krsnik, Z., Coppola, G., Bogdanovic, D., Geschwind, D.H., Mane, S.M., State, M.W., Sestan, N., 2009. Functional and evolutionary insights into human brain development through global transcriptome analysis. Neuron 62, 494–509.
Kasprian, G., Langs, G., Brugger, P.C., Bittner, M., Weber, M., Arantes, M., Prayer, D., 2011. The prenatal origin of hemispheric asymmetry: an in utero neuroimaging study. Cereb. Cortex Adv. Access 21 (5), 1076–1083.
Keller, S.S., Crow, T., Foundas, A., Amunts, K., Roberts, N., 2009. Broca's area: nomenclature, anatomy, typology and asymmetry. Brain Lang. 109, 29–48.
Kriegstein, A., Noctor, S., Martinez-Cerdeno, V., 2006. Patterns of neural stem and progenitor cell division may underlie evolutionary cortical expansion. Nat. Rev. Neurosci. 7, 883–890.
LeMay, M., 1984. Radiological developmental and fossil asymmetries. In: Geschwind, N., Galaburda, A.M. (Eds.), Cerebral Dominance. Harvard University Press, Cambridge, pp. 26–42.
Leroy, F., Mangin, J.F., Rousseau, F., Glasel, H., Hertz-Pannier, L., Dubois, J., Dehaene-Lambertz, G., submitted for publication. Atlas-Free Surface Reconstruction of the Cortical Grey–White Interface in Infants. PloS One.
Lohmann, G., von Cramon, D.Y., Steinmetz, H., 1999. Sulcal variability of twins. Cereb. Cortex 9, 754–763.
Mangin, J.F., Riviere, D., Cachia, A., Duchesnay, E., Cointepas, Y., Papadopoulos-Orfanos, D., Collins, D.L., Evans, A.C., Regis, J., 2004. Object-based morphometry of the cerebral cortex. IEEE Trans. Med. Imaging 23, 968–982.
Ochiai, T., Grimault, S., Scavarda, D., Roch, G., Hori, T., Riviere, D., Mangin, J.F., Regis, J., 2004. Sulcal pattern and morphology of the superior temporal sulcus. NeuroImage 22, 706–719.
Penhune, V.B., Zatorre, R.J., MacDonald, J.D., Evans, A.C., 1996. Interhemispheric anatomical differences in human primary auditory cortex: probabilistic mapping and volume measurement from magnetic resonance scans. Cereb. Cortex 6, 661–672.
Perani, D., Saccuman, M.C., Scifo, P., Spada, D., Andreolli, G., Rovelli, R., Baldoli, C., Koelsch, S., 2010. Functional specializations for music processing in the human newborn brain. Proc. Natl. Acad. Sci. U. S. A. 107, 4758–4763.
Régis, J., Mangin, J.F., Ochiai, T., Frouin, V., Rivière, D., Cachia, A., Tamura, M., Samson, Y., 2005. "Sulcal Root" generic model: a hypothesis to overcome the variability of the human cortex folding patterns. Neurol. Med. Chir. (Tokyo) 45, 1–17.
Rousseau, F., Glenn, O., Iordanova, B., Rodriguez-Carranza, C., Vigneron, D., Barkovitch, J., Studholme, C., 2006. Registration-based approach for reconstruction of high-resolution in utero fetal MR brain images. Acad. Radiol. 13, 1072–1081.
Sun, T., Patoine, C., Abu-Khalil, A., Visvader, J., Sum, E., Cherry, T.J., Orkin, S.H., Geschwind, D.H., Walsh, C.A., 2005. Early asymmetry of gene transcription in embryonic human left and right cerebral cortex. Science 308, 1794–1798.
Telkemeyer, S., Rossi, S., Koch, S.P., Nierhaus, T., Steinbrink, J., Poeppel, D., Obrig, H., Wartenburger, I., 2009. Sensitivity of newborn auditory cortex to the temporal structure of sounds. J. Neurosci. 29, 14726–14733.
Toga, A.W., Thompson, P.M., 2003. Mapping brain asymmetry. Nat. Rev. Neurosci. 4, 37–48.
Van Essen, D.C., 1997. A tension-based theory of morphogenesis and compact wiring in the central nervous system. Nature 385, 313–318.
Van Essen, D.C., 2005. A Population-Average, Landmark- and Surface-based (PALS) atlas of human cerebral cortex. NeuroImage 28, 635–662.
Vasung, L., Huang, H., Jovanov-Milosevic, N., Pletikos, M., Mori, S., Kostovic, I., 2010. Development of axonal pathways in the human fetal fronto-limbic brain: histochemical characterization and diffusion tensor imaging. J. Anat. 217, 400–417.
von Economo, C., Koskinas, D.N., 1925. Die cytoarchitektonik der Hirnrinde des erwachsenen menschen. Springer, Wien, Berlin.
Wada, J.A., Clarke, R., Hamm, A., 1975. Cerebral hemispheric asymmetry in humans. Cortical speech zones in 100 adults and 100 infant brains. Arch. Neurol. 32, 239–246.
Watkins, K.E., Paus, T., Lerch, J.P., Zijdenbos, A., Collins, D.L., Neelin, P., Taylor, J., Worsley, K.J., Evans, A.C., 2001. Structural asymmetries in the human brain: a voxel-based statistical analysis of 142 MRI scans. Cereb. Cortex 11, 868–877.
Witelson, S.F., Pallie, W., 1973. Left hemisphere specialization for language in the newborn: neuroanatomical evidence for asymmetry. Brain 96, 641–646.
Yakovlev, P.I., 1962. Morphological criteria of growth and maturation of the nervous system in man. Res. Publ. Assoc. Res. Nerv. Ment. Dis. 32, 3–46 (Baltimore, MD).
Yeni-Komshian, G.H., Benson, D.A., 1976. Anatomical study of cerebral asymmetry in the temporal lobe of humans, chimpanzees, and rhesus monkeys. Science 192, 387–389.
Yousry, T.A., Schmid, U.D., Alkadhi, H., Schmidt, D., Peraud, A., Buettner, A., Winkler, P., 1997. Localization of the motor hand area to a knob on the precentral gyrus. A new landmark. Brain 120, 141–157.
Zatorre, R.J., Belin, P., 2001. Spectral and temporal processing in human auditory cortex. Cereb. Cortex 11, 946–953.